Electronic Supplementary Information (ESI)

Carbon nanotubes decorated with zinc oxide quantum dots enables high-efficiency lithium-sulfur batteries

Rui Huang,‡[a] Wei Mao,‡[b] Yi Hu,[a] Xifang Chen,[c]* Xuan Cao,[b] Paul Takyi-Aninakwa,[a] Bo Zhao,[a] Lixian Song,[a] Haitao Hu[d,e]* and Yingze Song[a]*

[a] *School of Materials and Chemistry, State Key Laboratory of Environment-Friendly Energy Materials, Southwest University of Science and Technology, Mianyang 621010, China.*
[b] *National Laboratory of Solid-State Microstructures, Jiangsu Key Laboratory of Artificial Functional Materials, College of Engineering and Applied Sciences and Collaborative Innovation Center for Advanced Microstructures, Nanjing University, Nanjing 210093, China.*
[c] *School of Chemistry & Chemical Engineering, Guangdong Provincial Key Lab of Green Chemical Product Technology, State Key Laboratory of Pulp and Paper Engineering, South China University of Technology, Guangzhou 510640, China.*
[d] *Spallation Neutron Source Science Center, Guangdong Provincial Key Laboratory of Extreme Conditions, Dongguan 523083, China.*
[e] *Institute of High Energy Physics, Chinese Academy of Sciences (CAS), Beijing 100049, China.*

Corresponding authors: yzsong@swust.edu.cn (Y. Song); chenxifang@swust.edu.cn (X. Chen); huht@ihep.ac.cn (H. Hu)

Keywords: Lithium-sulfur batteries, zinc oxide quantum dots, carbon nanotubes, conductivity-polarity coupling, sulfur reaction kinetics

1. ***Experimental Section***

1.1 *Synthesis of ZnO quantum dots*

0.176 g of zinc acetate dihydrate was dissolved in 40 mL of anhydrous ethanol under magnetic stirring. 0.089 g of potassium hydroxide was dissolved in 40 mL of anhydrous ethanol until full dissolution. The resulting two solutions were mixed and transferred into a three-necked flask. The reaction system was kept at 75 oC for 20 min under a continuous argon flow. Then, the system was rapidly cooled by immersing the flask in an ice bath. ZnO quantum dots were finally obtained via centrifugation at 10000 rpm. Due to the loss of some smaller quantum dots during the centrifugation process, approximately 0.06 g of quantum dots were ultimately obtained.

1.2 *Synthesis of ZnO@CNT*

0.5 g of CNT with oxygen-containing groups and 2 g of ZnO quantum dots-ethanol solution were added into 20 mL glass vial. Then, an additional 8 g of anhydrous ethanol was introduced.

The mixture was subjected to magnetic stirring for 24 h, followed by drying. The dried product was subsequently ground to finally obtain 0.5038 g of ZnO@CNT.

1.3 *Preparation of ZnO@CNT separator*

90 mg of ZnO@CNT (or CNT or ZnO) and 10 mg of polyvinylidene fluoride (PVDF) binder were uniformly mixed in N-methyl pyrrolidone (NMP) solvent to generate a homogeneous slurry. Subsequently, the slurry was coated onto the surface of the PP separator using a scraper. The coated separator was then placed in a vacuum oven at 60 °C for 12 h to pledge full solvent evaporation. Finally, the dried separator was punched into disks with a diameter of 19 mm prior to use.

1.4 *Preparation of sulfur/carbon cathodes*

Nano sulfur powder and Super P were uniformly mixed at a mass ratio of 3:1. Then, the mixture was sealed into a glass vial, and heated at 155 °C for 6 h. After cooling to room temperature, the resulting composite was further ground. Next, the sulfur/carbon composite, Super P, and PVDF binder were mixed at a mass ratio of 8:1:1 to form a viscous slurry. The prepared slurry was coated on the surface of the aluminum foil, followed by drying in a vacuum oven at 60 °C for 12 h. Finally, the cathode film was punched into small disks with a diameter of 13 mm. The mass content of sulfur in the entire cathode is around 60 wt.%.

1.5 *Material characterizations*

The detailed morphologies and element distribution of the samples were observed by aberration-corrected transmission electron microscope (FEI Titan Cubed G2 60-300, Netherlands) and field emission scanning electron microscope from (MAIA3 model 2016, Czech). X-ray photoelectron spectrometer (Thermo ESCALAB 250XI, America) was performed to detect the surface chemical compositions of samples. N_2 adsorption and desorption isotherms of sample was performed on Surface area and pore analyzer (Quantachrome Autosorb-IQ, America). The ultraviolet−visible absorption spectra were recorded using a dual-beam ultraviolet−visible spectrometer (TU-1901, China).

1.6 *Permeation and adsorption tests*

Lithium sulfide and sublimated sulfur at a molar ratios of 1:3 and 1:5 were respectively dissolved in DME solvents to obtain Li_2S_4 and Li_2S_6 solutions. For the permeation tests, ZnO@CNT and CNT based separators were placed into the caps of inner bottle in bottle-in-bottle devices. The inner and outer bottles were filled with 2 mL of Li_2S_4 solution and 2 mL of DME solvent, respectively. For the adsorption tests, 20 mg of ZnO@CNT and CNT were added to two bottles with 2 mL of Li_2S_6 solution. All the operations were conducted in an argon-filled glovebox.

1.7 *Li_2S nucleation/dissociation tests*

First, lithium sulfide and sublimated sulfur were reacted at a molar ratio of 1:7 to obtain a Li_2S_8 solution. Then, carbon paper (CP) was punched into small discs with a diameter of 13 mm, followed by covering 0.2 mg of ZnO@CNT (or CNT). Cells were assembled by using the prepared CP-ZnO@CNT (or CP-CNT) as the cathode, 20 µL of Li_2S_8 solution as the catholyte, commercial PP film (Celgard 2500) as the separator, lithium foil as the anode, and 20 µL of DME/DOL solvent (*v*:*v*=1:1) containing 1.0 mol L^{-1} LiTFSI and 2.0 wt.% $LiNO_3$ as the anolyte. For the Li_2S nucleation tests, the cells were first discharged at 0.112 mA to 2.06V, and then continued to discharge at 2.05 V until the current was less than 10^{-5} A. Similarly, the dissociation tests were first discharged at 0.112 mA to the voltage below 1.7 V, and then potentiostatically charged at 2.35 V till the current was lower than 10^{-5} A. All the Li_2S nucleation/decomposition tests were performed on an electrochemical analyzer (LANHE M340A, China). Finally, the nucleation/decomposition capacities of Li_2S on substrates were calculated according to the Faraday's law.

1.8 *Electrochemical performance tests*

Coin-type LSBs were assembled with sulfur/carbon cathodes, ZnO@CNT based separator, lithium foils, and electrolyte. The electrolyte was 1,2-dimethoxyethane (DME)/1,3- dioxolane (DOL) solvent (v: v=1:1) containing 1.0 mol L^{-1} LiTFSI and 2.0 wt.% $LiNO_3$. The sulfur mass loadings for routine and high-load coin-type batteries are respectively around 1.5 and 4.7 mg cm^{-2}. And the electrolyte/sulfur (E/S) ratios are 15.0 and 8.0 μL mg_S^{-1}, respectively. The sulfur mass loading and the corresponding E/S ratio for the single-layer pouch cell are 1.6 mg cm^{-2} and 14.0 μL mg_S^{-1}, respectively. Battery testing system (NEWARE CT4008, China) was used to test the rate and cycling performance of coin-type batteries and soft-packaged pouch cell within the voltage window of 1.7–2.8 V. Cyclic voltammetry curves of LSBs were recorded on the electrochemical workstation (Metrohm Autolab G204, Switzerland).

1.9 *Theoretical calculations*

Density functional theory (DFT) calculations were performed using the Vienna ab initio simulation package (VASP) [1] with the exchange-correlation function of Perdew-Burke-Ernzerhof. The electron-ion interaction was considered in the form of the projector augmented wave method (PAW) [2, 3]. Energy cutoff of 400 eV for the plane wave basis set was used for the structure optimization and transition states search. The Brillouin zone was sampled using a 3×3×1 Monkhorst-Pack k-point mesh. The total energy convergence and the forces on each atom were set to be lower than 10−5 eV and 0.02 eV A−1. The adsorption energy (Eads) of the polysulfides on Graphene or ZnO (002) substrates was calculated as following:

$$E_{ads} = [E(surface) + E(Li_2S_n)] - E(system)$$

Where $E(surface)$ is the energy of the clean substrate, $E(Li_2S_n)$ is the energy of the isolated polysulfides, and $E(system)$ is the energy of the polysulfides adsorbed on the substrate.

2. *Figures*

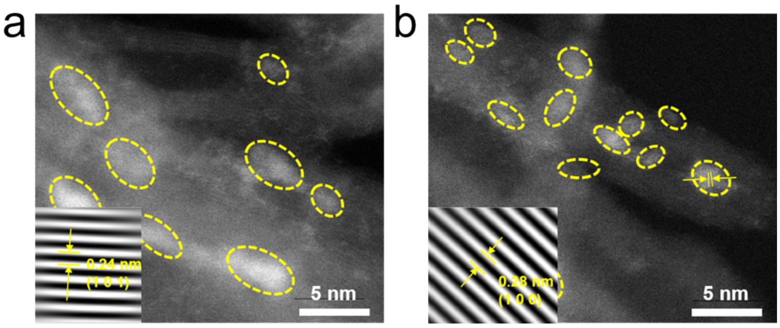

Fig. S1. HRTEM images of ZnO@CNT.

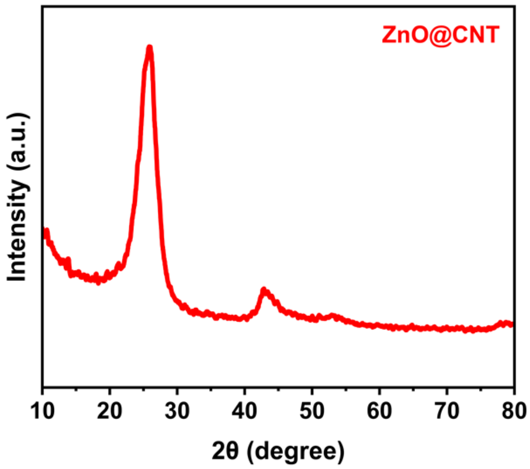

Fig. S2. XRD pattern of ZnO@CNT.

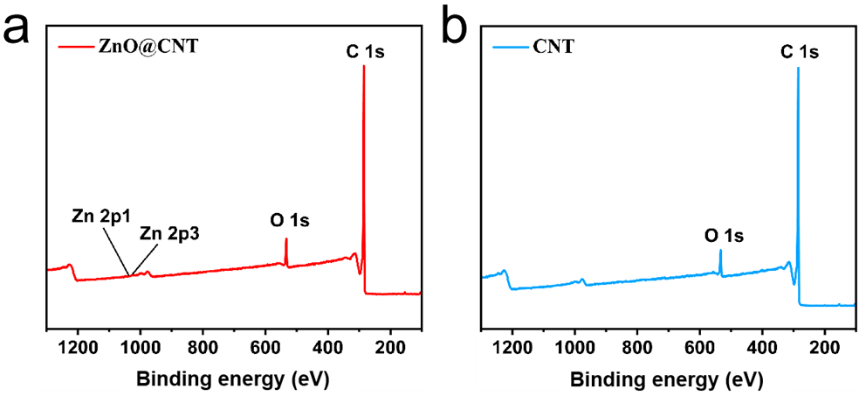

Fig. S3. The XPS full spectra of (a) ZnO@CNT and (b) CNT.

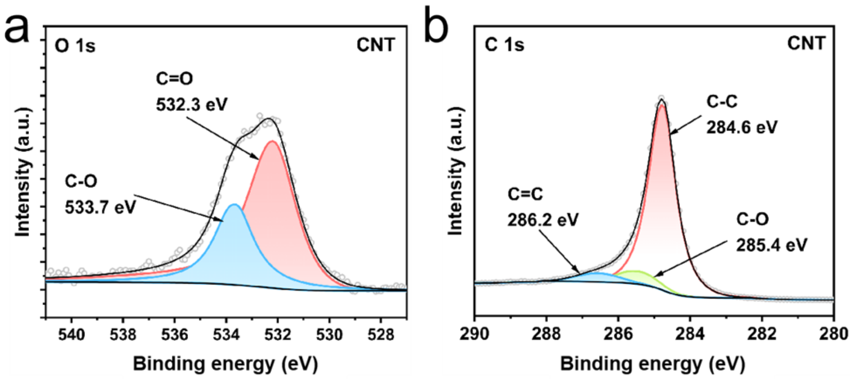

Fig. S4. High-resolution (a) O 1s and (b) C 1s XPS spectra of CNT.

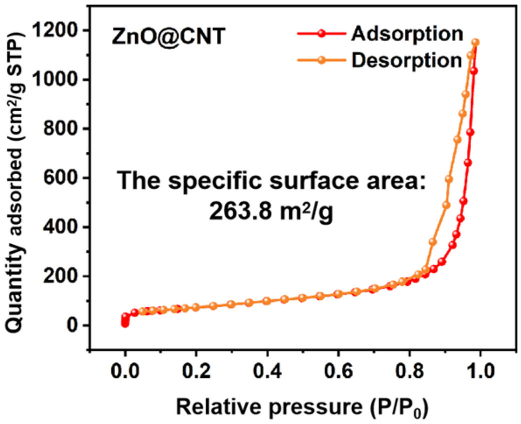

Fig. S5. N_2 adsorption and desorption isotherms of ZnO@CNT.

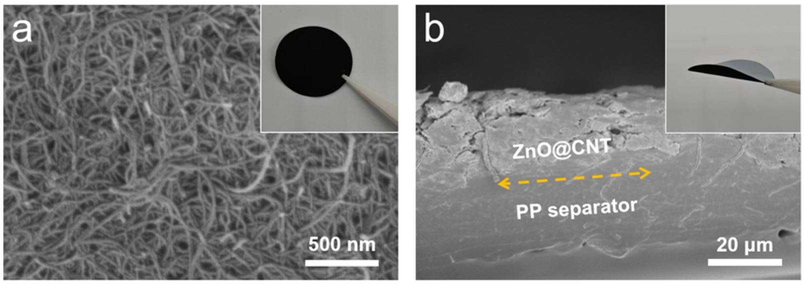

Fig. S6. SEM images of the ZnO@CNT based separator with the insets showing its digital photographs.

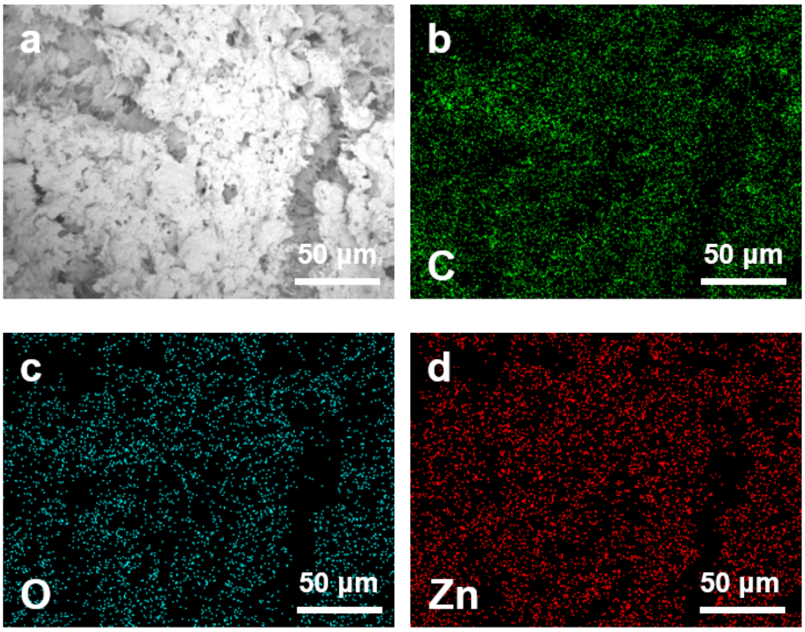

Fig. S7. SEM and mapping images of ZnO@CNT based separator.

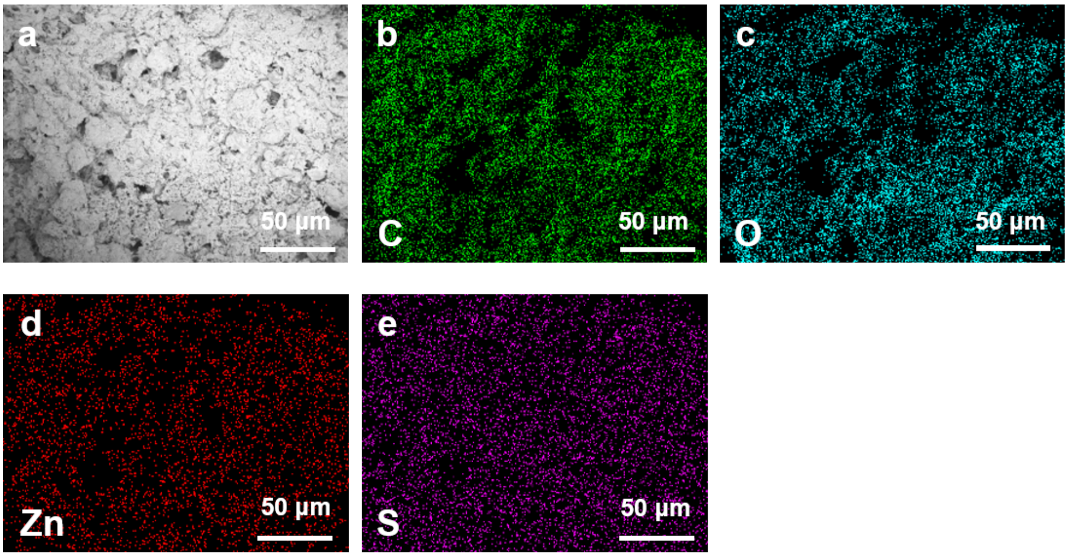

Fig. S8. SEM and mapping images of ZnO@CNT based separator after permeation tests.

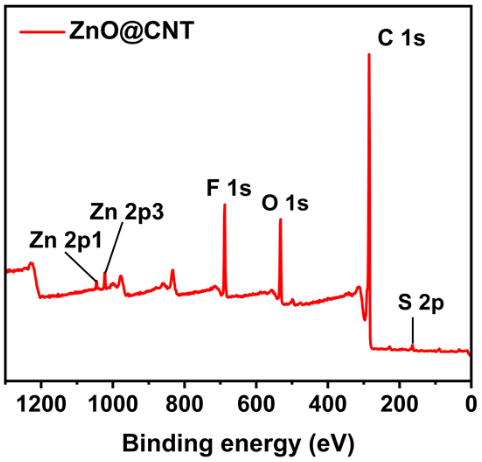

Fig. S9. The full XPS spectrum of ZnO@CNT after adsorption experiments.

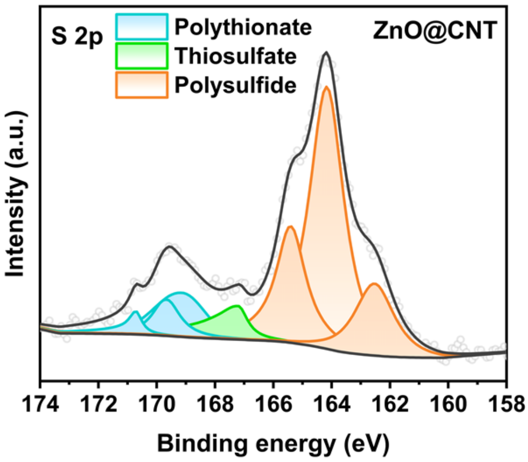

Fig. S10. High-resolution S 2p XPS spectrum of ZnO@CNT after Li_2S_4 permeation tests.

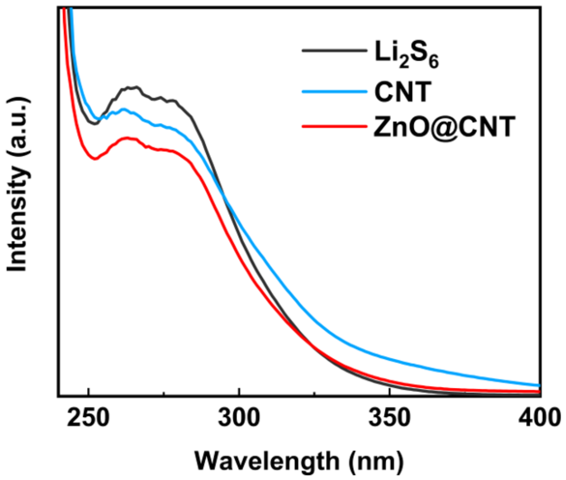

Fig. S11. UV–vis absorption spectra of a Li_2S_6 solution after adsorption experiments.

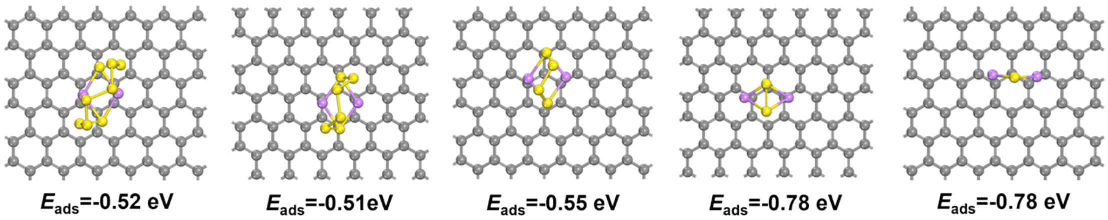

Fig. S12 Adsorption energies and optimal geometric configurations of CNT for Li_2S_8, Li_2S_6, Li_2S_4, Li_2S_2, and Li_2S.

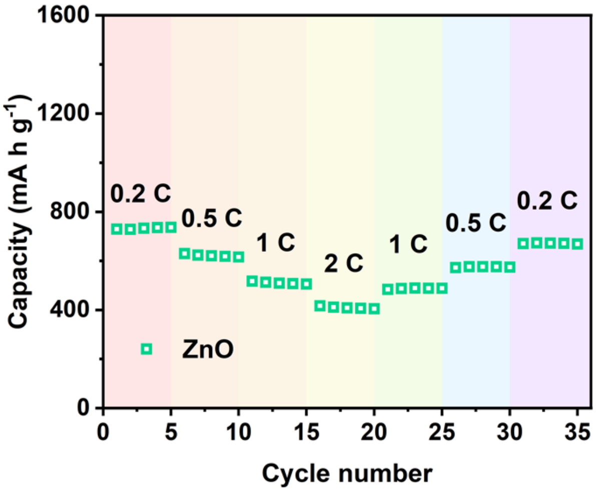

Fig. S13. Rate capacities of batteries with ZnO particles-based separator.

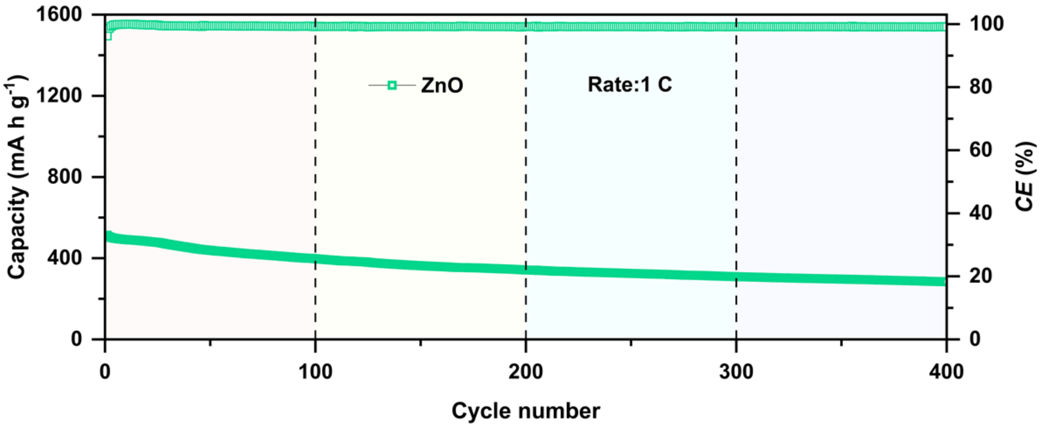

Fig. S14. Long-term cycling performance of battery with ZnO particles-based separator at 1 C.

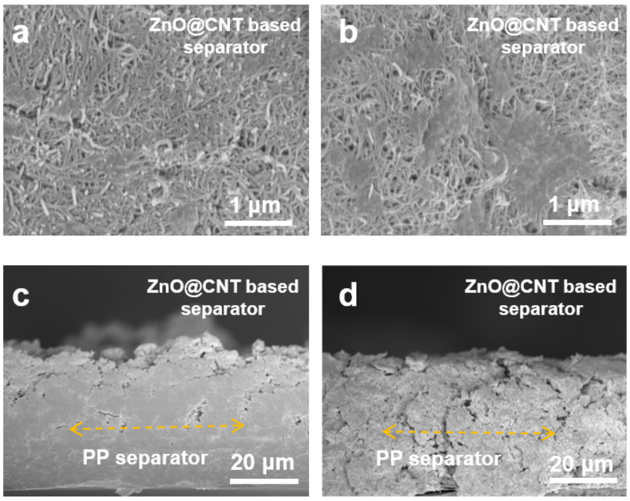

Fig. S15. SEM images of the ZnO@CNT based separator (a, c) before and (b, d) after cycling for 100 cycles at 1 C.

Table. S1. Performance comparison of pouch cells using ZnO@CNT composites with previously reported pouch cells.

Literature	S mass loading (mg cm^{-2})	E/S ratio (μL mg_S^{-1})	Rate (C)	Initial capacity (mA h g^{-1})	Cycle number
This work	1.6	14	0.2	1080.33	150
Ref. [4]	1.3	/	0.1	～1150	100
Ref. [5]	1.5	20	0.1	1353.2	170
Ref. [6]	3.5	9.5	0.2	809.23	50
Ref. [7]	/	7	0.5	952.6	100
Ref. [8]	5.6	8.6	0.05	729	30
Ref. [9]	1.4	10	1	692.1	100
Ref. [10]	5.4	4.6	0.1	956	50
Ref. [11]	/	12	0.2	882.1	100
Ref. [12]	1.4	15	0.1	1164	50
Ref. [13]	2.2	10	0.1	～550	100

References

1. G. Kresse, *et al. Comput. Mater. Sci.*, 1996, **6**, 15–50.
2. G. Kresse, *et al. Phys. Rev. B*, 1996, **54**, 11169–11186.
3. J. P. Perdew, *et al. Phys. Rev. Lett.*, 1996, **77**, 3865−3868.
4. M. Wang, *et al. Adv. Funct. Mater.,* 2022, **33**, 2211978.
5. Q. Shao, *et al. J. Energy Chem.*, 2020, **51**, 262–271.
6. Z. He, *et al. Chem. Eng. J., 2*022, **448**, 137656.
7. R. Yang, *et al. Chem. Commun.,* 2024, **60**, 9078–9081.
8. H. Wang, *et al. Electrochim. Acta*, 2021, **403**, 139644.
9. R. Yang, *et al. Rare Met.*, 2024, **43**, 2842–2850.
10. F. Ma, *et al. Chem. Eng. J.,* 2023, **459**, 141526.
11. S. Yu, *et al. Nano Energy*, 2021, **89**, 106414.
12. Q. Yang, *et al. Nano Energy*, 2022, **452**, 139638.
13. A. K. Das, *et al. ACS Appl. Mater. Interfaces*, 2025, **17**, 7657–7669.